4

A Method for the Evaluation of Bone Specimen Material Properties

by

Robert H. Hopper, Jr.

Piziali & Associates

James H. McElhaney and Barry S. Myers

Department of Biomedical Engineering and
Division of Orthopaedic Surgery
Duke University

Paper was presented at the 23rd International Workshop on Human Subjects for Biomechanical Research. This paper has not been screened for accuracy nor refereed by any body of scientific peers and should not be referenced in the open literature.

Abstract

This study discusses a general technique to assess the material properties of bone specimens which can be utilized to determine parameters for a variety of material models. The technique experimentally quantifies the three-dimensional specimen geometry and evaluates the mechanical response of the bone to a well-defined loading condition. Bone specimen geometry is then used to construct a finite element mesh. Principal surface strains derived from strain gauge rosettes bonded to the bone surfaces are subsequently utilized to evaluate material properties using an inverse finite element technique. Material model parameters are optimized for a particular type of material model based on the minimization of a least squares error criteria. In the present study, bone specimens are taken from the posterior aspect of the occiput and loads are imposed using four-point bending. To avoid structural degradation associated with machining small specimens, large bone specimens are utilized. The experimental results are used to determine the degree to which isotropic, linearly elastic models can be used to characterize the experimental data. The material property parameters derived from the finite element models are also compared against material properties derived from elementary beam bending theory.

The experimental results indicate that the occipital bone specimens exhibit strongly linear mechanical responses over the range of strains and loading rates considered in the present study. Characterizing the bone as a homogeneous, linearly elastic, isotropic material and using an inverse finite element analysis yields a mean Young's modulus of 16.9 $\pm$ 5.3 GPa and a mean Poisson's ratio of 0.355 ± 0.081. These values are in close agreement with material properties for cortical bone derived from other locations of the skull. The error between experimentally measured surface strains and those predicted by the finite element simulations, using optimal material properties, is found to be on the order of 10%. The material properties predicted by elementary beam bending equations often did not agree well with. the results from the finite element simulations. However, inter-specimen material property variations were also significant in the present study and tended to obscure variations stemming from the different analysis techniques.

Introduction

The purpose of this investigation is to develop and apply a general technique that can be used to evaluate the material constants associated with any arbitrary model chosen to represent the constitutive behavior of bone. In this study, a series of bone specimen tests was undertaken to obtain data that could be used to determine constitutive relationships for basilar skull bone. While the literature provides a foundation for material characterizations of bone from various anatomic locations, the irregular geometry associated with basilar skull bone has discouraged experimental characterization of its material properties.

Literature Review

The majority of studies devoted to assessing the material properties of bone have employed either mechanical or ultrasonic techniques. Mechanical testing typically relies on the application of measurable loads to specimens machined to uniform dimensions. Measured deformations are used to calculate strains and mechanical properties including elastic modulus, yield strength, and ultimate strength are determined. It is generally accepted that for the determination of an elastic modulus, machining tends to degrade the specimen, resulting in under-estimation of the modulus, while frictional and end-effects tend to stiffen the specimen, leading to an over-estimation of the modulus (Keaveny and Hayes, 1993). The magnitude of these artifacts is often difficult to assess (Keaveny *et al.*, 1993). To characterize each independent material constant for a particular model, a separate test is often required. ASTM standards (ASTM, 1978) provide a foundation for most testing techniques but often require modifications in view of specimen geometry.

Ultrasonic techniques rely on the premise that elastic modulus, E, is directly related to material density, ρ, and the velocity of wave propagation, υ, according to equations of the general form $E = \rho\upsilon^2$. The exact relationship between wave speed, density, and modulus depends on the mode of wave propagation, wavelength, and the cross-section of the material through which the wave propagates. Elastic wave theory predicts closed form relationships between stress wave velocities and anisotropic elastic properties for materials with at least orthotropic symmetry (Ashman, 1989). Elastic moduli determined by ultrasonic techniques have been shown to compare well with those measured by mechanical testing techniques (Ashman, *et al.* 1984; Ashman *et al.*, 1987). The major disadvantage of ultrasound is that it cannot be used to directly measure strength or loading rate-dependent properties.

While many studies have characterized the mechanical properties of bone specimens from various anatomic locations, only a few studies have been devoted to the skull. One of the earliest studies characterizing the mechanical properties of skull bone was performed by Evans and Lissner (1957). They found that the average ultimate strength of specimens of parietal compact bone was 70 MPa in tension and varied from 152 to 167 MPa in compression depending on the loading direction. The average compressive strength of cancellous diploe bone was reported to be 25 MPa. Wood (1971) investigated the mechanical properties of unembalmed human cranial bone in tension and performed tests on over 120 specimens from thirty subjects. The specimens

were taken from the compact layers of parietal, temporal, and frontal bone and tested at strain rates ranging from static to 150 sec^{-1}. The modulus of elasticity, breaking stress, and strain were found to be strain-rate sensitive, while the energy absorbed to failure was not. The modulus of elasticity ranged from 12 to 20 GPa, and the average strain energy density at failure was 347 kJ/m^3. At low strain rates, the average tensile strength was found to be 69 MPa and agrees closely with the values obtained by Evans and Lissner (1957). McElhaney *et al.* (1970) examined the compressive properties of machined bone specimens taken from human femora, vertebrae, and cranial bone. Cuboidal specimens were prepared by wet grinding. For cranial compact bone, a modulus of 12.5 ± 4.1 GPa and a Poisson's ratio of 0.28 ± 0.04 was reported. The ultimate strength was found to be 144 ± 47 MPa. More recently, Dechow *et al.* (1993) have determined the orthotropic elastic constants for human craniofacial bone specimens obtained from the supraorbital region and the buccal surface of the mandible of unembalmed cadavers using an ultrasonic pulse transmission technique in three mutually perpendicular directions.

Methods

An apparatus was constructed to apply four-point bending and is illustrated in Figure 1. Incorporating vertically aligned U-joints above and below the specimen and loading the fixturing in tension insured that the resultant force applied to the bone specimen was vertical. To closely control the regions of load application, knife-edge supports were incorporated in the fixture design.

Six occipital bone specimens were obtained from unembalmed cadaveric heads. Each cadaver head was removed from the freezer and allowed to equilibrate with ambient room temperature in a 100% relative humidity environment. Soft tissue was removed from the occipital region and specimens were removed from the skull using a Stryker saw. Care was taken to insure that pre-existing fractures in the bone specimens did not exist. After each specimen was obtained, a uniform rectangular grid was marked on both the upper and lower bone surfaces at 0.508 cm intervals. The upper bone surface corresponded to the anatomic exterior of the skull while the lower bone surface corresponded to the interior of the skull. The bone specimens were then ground to a width of 2.54 cm and a length that was a multiple of 0.508 cm, typically between 7.62 and 10.16 cm. Subsequently, both bone surfaces were digitized at grid line intersections with the aid of a Craftsman Model 38674 dial gauge. Measurements along the thickness of each specimen were made with Craftsman Model 40181 calipers. The accuracy of both the dial gauge and calipers was 0.00254 cm.

To create uniform surfaces for loading, rectangular blocks were cast on each end of the bone specimen using Southern Prosthetics Supply 087-0880 polyester resin. At each end of the specimen, 2.032 cm of bone was embedded in the polyester resin. Once the ends of the bone specimens were cast, the exposed surfaces of the resin were either sanded or machined to produce smooth, uniform bearing surfaces.

For each specimen, strain gauge rosettes were mounted on both the upper and lower surfaces. In the first test, planar rosettes (Micro-Measurements CEA-13-062UR-350), with

gauges oriented at 45 degrees with respect to each other, were used to measure strain. In subsequent tests, stacked rosettes (Micro-Measurements WK-06-060WR-350), with gauges oriented at 45 degrees with respect to each other, were utilized. To limit local heating, gauge excitation was limited to 2.0 Volts for the stacked rosettes.

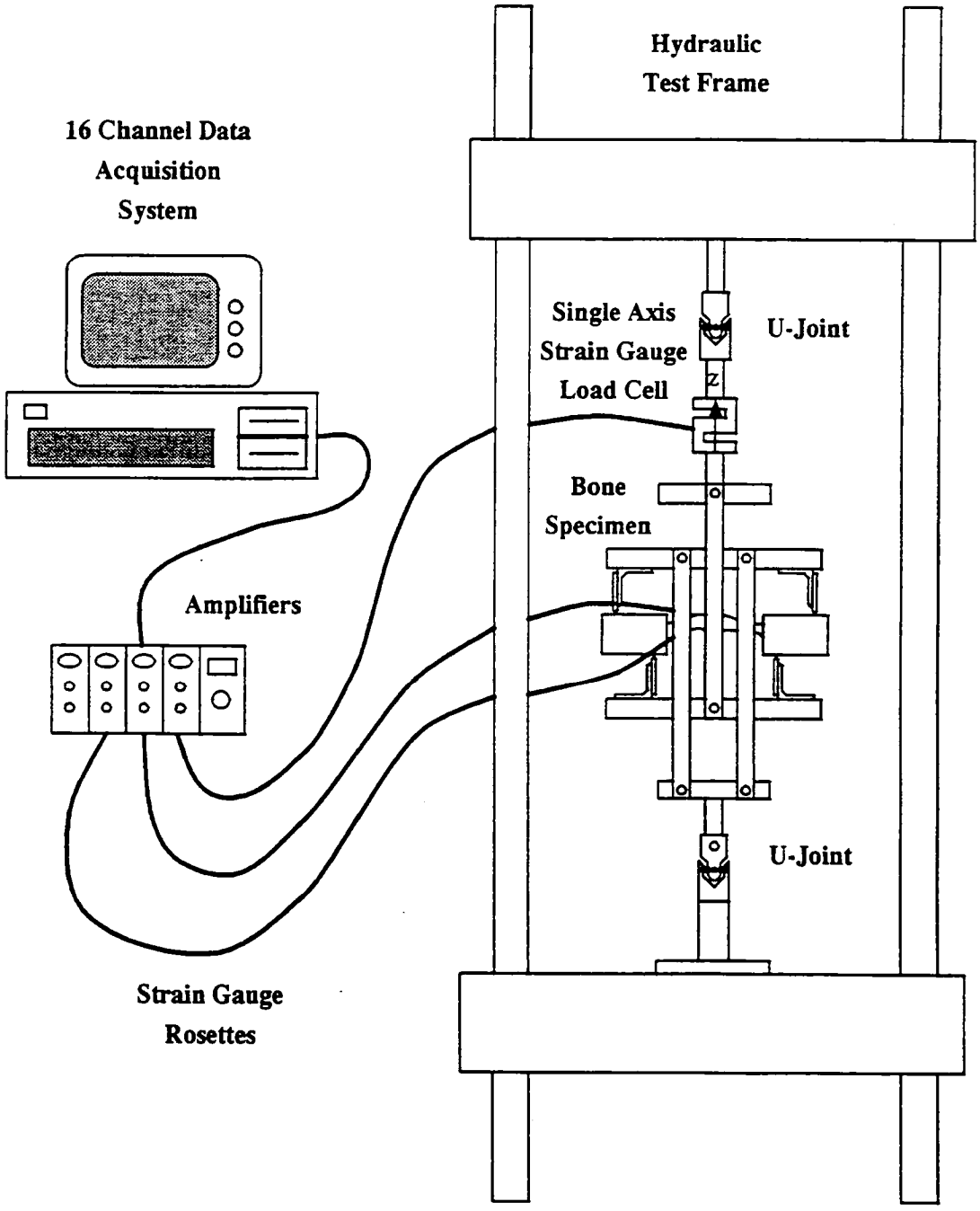

Figure 1. Experimental apparatus used for four-point bending tests. Strain gauge rosettes were bonded to the upper and lower surfaces of each test specimen. Loads were applied by moving the hydraulic ram downward at a constant velocity.

Load application regions were defined symmetrically on the castings of each bone specimen and the four-point bending jig was adjusted to match these dimensions. The knife-edge supports, defining the regions of load application, were typically spaced 2.54 - 3.55 cm apart on the castings to create a sufficiently large moment without subjecting the polyester blocks to large shear forces. Once the specimen had been oriented in the test frame, the strain gauge leadwires were connected to terminal strips that led to Micro-Measurements Model 2120 strain gauge conditioners. Each gauge was connected in a quarter-bridge configuration and transient signal fluctuations associated with thermal heating were allowed to equilibrate. Tests were performed by subjecting the hydraulic ram to a constant velocity ramp displacement. Digital data acquisition was accomplished with an RC Electronics Computerscope using eight channels of data dedicated to load, ram displacement, and six channels of strain gauge data. Four thousand uniformly sampled data points were used to characterize each channel of data. All tests were non-destructive. After each test, data was uploaded to a Sun SPARCstation 2 for analysis.

A finite element model of the bone specimen embedded in the polyester resin was constructed based on the digitized bone surfaces and dimensions of the polyester blocks. The experimentally measured force was equally distributed between both supports on the upper surface of the resin and uniformly applied along the line of the knife-edge contact. One side of the lower casting surface was constrained only in the direction of the ram displacement while the other surface was completely constrained to eliminate any rigid body modes in the model. Principal surface strains were computed from the experimental data and used to validate the principal strains obtained from the simulations. Linearly elastic, isotropic material models were used to represent bone. The mechanical response of the polyester resin was determined using rectangular, prismatic specimens instrumented with strain gauges on the upper and lower surfaces and subject to four-point bending. The polyester was considered to be a linearly elastic, isotropic material and elementary beam theory was used to evaluate material properties.

As the material property parameters of each bone specimen were iteratively adjusted, experimentally measured surface strains were compared with principal surface strains predicted by the simulations. For the computational models, surface strains were derived by extrapolating element strains to the bone surface. In the event that a rosette covered multiple elements, the capacity to weight the principal strains from each element in the computation of the resultant surface strain was incorporated. These strains were then compared to the experimental strain values and a percent difference was computed using the expression

$$\text{error}_i = \left(\frac{\varepsilon_{\text{fem}_i} - \varepsilon_{\text{exp}_i}}{\varepsilon_{\text{exp}_i}} \right) \text{x } 100\%$$

where ε_{exp} is the experimental strain and ε_{fem} is the strain predicted by the simulation.

The overall agreement between experimental and simulation data was evaluated using several error criteria, including average absolute error, average squared error, weighted absolute error, and weighted squared error. Average absolute error and average squared error are defined as

$$\text{Average Absolute Error} = \frac{1}{n}\sum_{i=1}^{n} \left| \text{error}_i \right| \text{ and}$$

$$\text{Average Squared Error} = \sqrt{\frac{1}{n}\sum_{i=1}^{n} (\text{error}_i)^2} .$$

To more heavily weight the dominant strain components, a weighting function defined as

$$w_i = \frac{\varepsilon_{\exp_i}}{\sum_{i=1}^{n} \varepsilon_{\exp_i}}$$

was incorporated to assess error, yielding the expressions

$$\text{Weighted Absolute Error} = \sum_{i=1}^{n} \left| w_i \text{ error}_i \right| \text{ and}$$

$$\text{Weighted Squared Error} = \sqrt{\sum_{i=1}^{n} w_i (\text{error}_i)^2} .$$

Optimal material properties for each specimen were based on the parameters that resulted in a minimum weighted squared error.

Results

While the same type of polyester was utilized in all of the bone specimen testing, it came from two different lots resulting in different mechanical properties. As a consequence, a single four-point bending tests was performed to characterize the mechanical response of each polyester resin lot. The polyester resin from the first lot, designated as Resin 1, was used for Bone Specimen Tests 1, 2, 3, and 4. The specimen cast for the bending tests was 3.64 cm wide, 1.21 cm in height, and 14.9 cm long. The force-strain data from both the upper and lower rosettes may be found in Figure 2. An equivalent moment may be determined by dividing the force value by two and multiplying by the distance separating the knife-edge supports on each resin block. In this test, the supports were separated by 2.54 cm. The experimental strain data exhibits a distinctly linear response and regression analyses indicated that the variation in principal surface strains with applied moment was 258 με/N-m and -97.0 με/N-m for the upper rosette. The lower rosette reflected values of 88.5 με/N-m and -311 με/N-m. Using an average strain based on the maximum principal strain from the upper rosette and the absolute value of the minimum principal strain from the lower rosette, a modulus of 3.97 GPa was calculated. The difference between the average strain and the largest magnitude principal strain values from the upper and lower rosettes was 9.28%. A Poisson ratio corresponding to both the upper and lower rosette data was calculated based on the ratio of the principal strains. The Poisson ratio for the polyester specimen, based on the average, was found to be 0.33. The ratios calculated for the upper and lower surfaces differed from the mean by 13.8%.

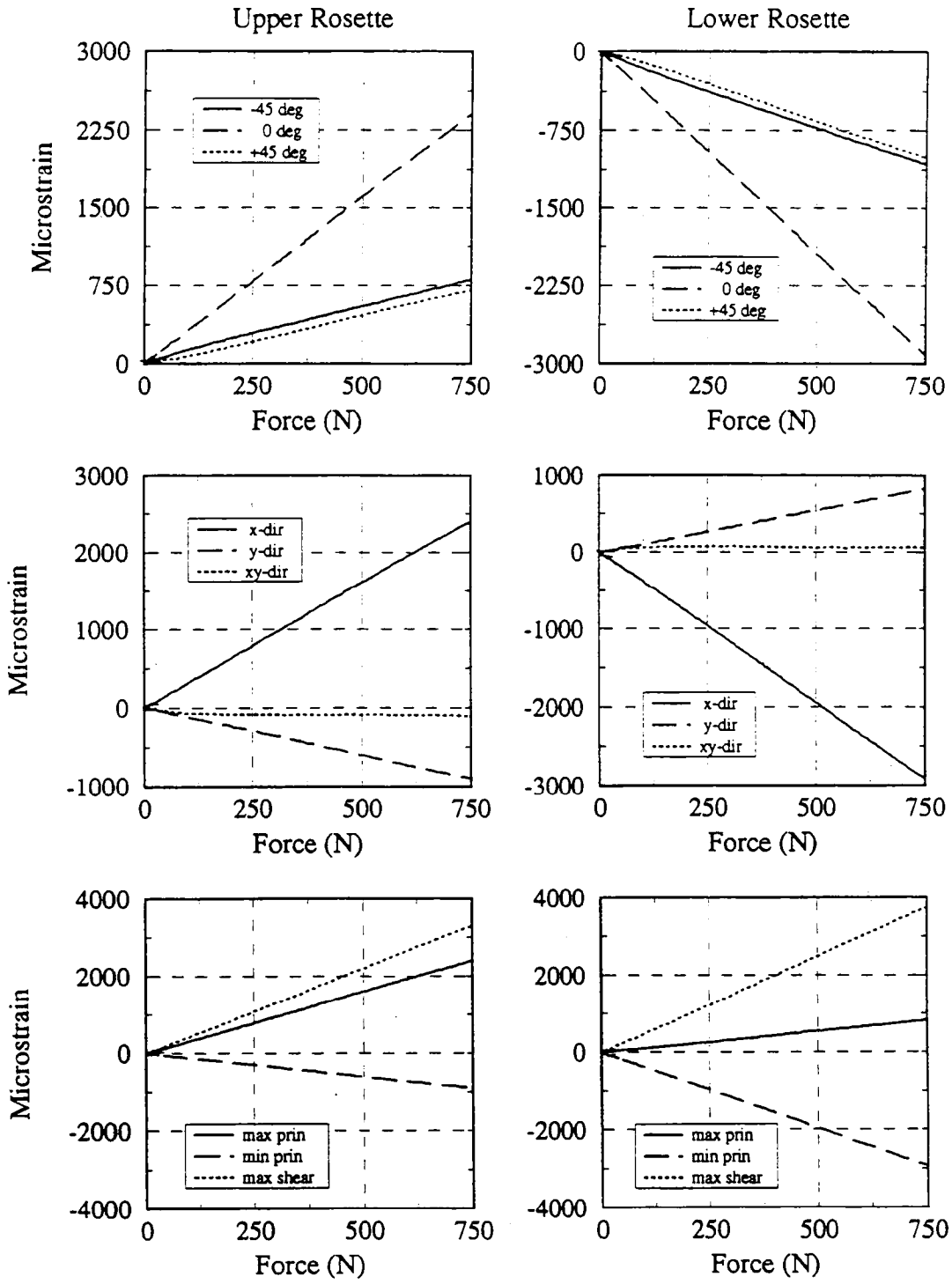

Figure 2. Force-strain data for rosettes bonded to the upper and lower surfaces of a rectangular specimen cast using Polyester Resin 1. Data is reported to peak force for the loading phase.

The polyester resin from the second lot, designated as Resin 2, was used for Bone Specimen Tests 5 and 6. The specimen cast for the bending tests was 4.44 cm wide, 0.785 cm in height, and 15.7 cm long. The force-strain data from both the upper and lower rosettes are illustrated in Figure 3. The distance separating the knife-edge supports on each side of the specimen was 3.048 cm for this test. Regression analyses indicated that the variation in principal surface strains with applied moment was 745 με/N-m and -253 με/N-m for the upper rosette. The lower rosette reflected values of 250 με/N-m and -767 με/N-m. The polyester modulus was found to be 2.90 GPa. The difference between the average strain and the largest magnitude principal strain values from the upper and lower rosettes was 1.47%. The average Poisson ratio for the specimen was found to be 0.33. The ratios calculated for the upper and lower surfaces differed from the mean by 1.94%.

The geometries of the occipital bone specimens imbedded in the polyester castings are depicted in Figures 4 and 5. Experimental force-strain curves to maximum load are illustrated in Figures 6 - 11. When resolving the gauge strains into normal and shearing components, the x-axis corresponded to the long axis of the bone specimen. To convert the force data to an equivalent moment, the force values should be divided by two and multiplied by the distance separating the knife-edge supports on each of the polyester blocks. In tests of Specimens 1 and 4, that distance was 2.54 cm. For Bone Specimens 2, 3, 5, and 6, the support separation was 3.048 cm.

In view of the linear nature of the mechanical behavior, a linear regression, ignoring initial transients, was used to derive the slope of each response. The slope was used to characterize each of the strain components by a single parameter. Table 1 summarizes the slopes of the principal strain-moment responses for the experimental gauge data from both the upper and lower rosettes of each bone specimen. Principal strain-moment values derived from optimal finite element simulations using linearly elastic, isotropic, homogeneous material models are also tabulated and the percent error between the predicted and experimental strains is calculated. Table 2 lists the optimal elastic constants based on the finite element simulations for each specimen and the associated errors using different error evaluation techniques detailed in the Methods section. Among the occipital bone specimens, the mean Young's modulus was found to be 16.9 ± 5.3 GPa while Poisson's ratio averaged 0.355 ± 0.081. Table 3 lists the elastic constants for each of the bone specimens based on both elementary beam bending and finite element results. Beam bending equations consistently predict lower modulus values based on the rosette data from the lower surface of the bone specimen, yielding a mean modulus of 9.4 ± 3.7 GPa. The data from the upper rosettes tend to predict higher modulus values, averaging 18.2 ± 2.7 GPa. Averaging the upper and lower rosette data yields a mean modulus of 13.8 ± 5.6 GPa. Using both the upper and lower surface strain data, beam theory predicts an average Poisson's ratio of 0.413 ± 0.115.

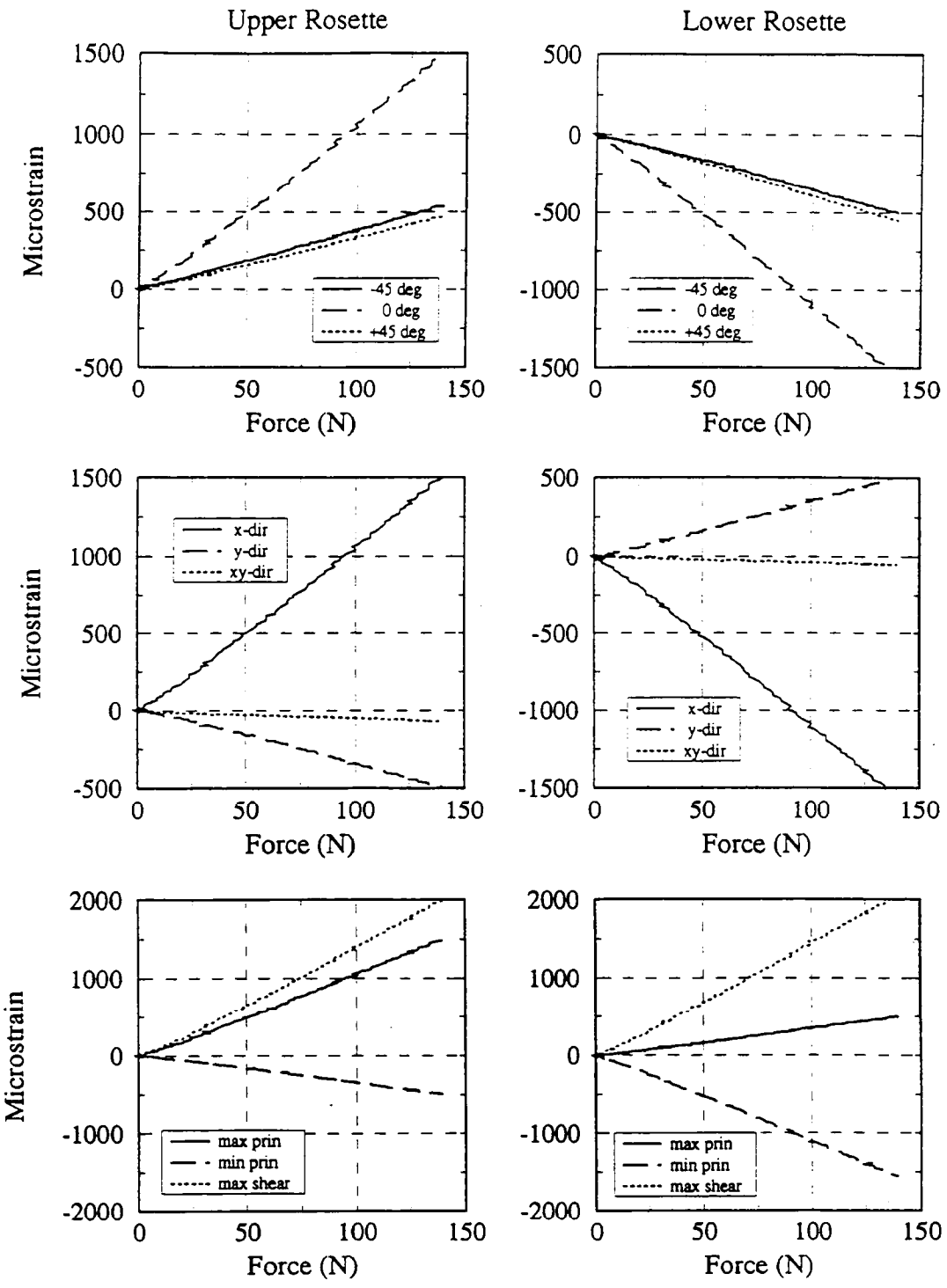

Figure 3. Force-strain data for rosettes bonded to the upper and lower surfaces of a rectangular specimen cast using Polyester Resin 2. Data is reported to peak force for the loading phase.

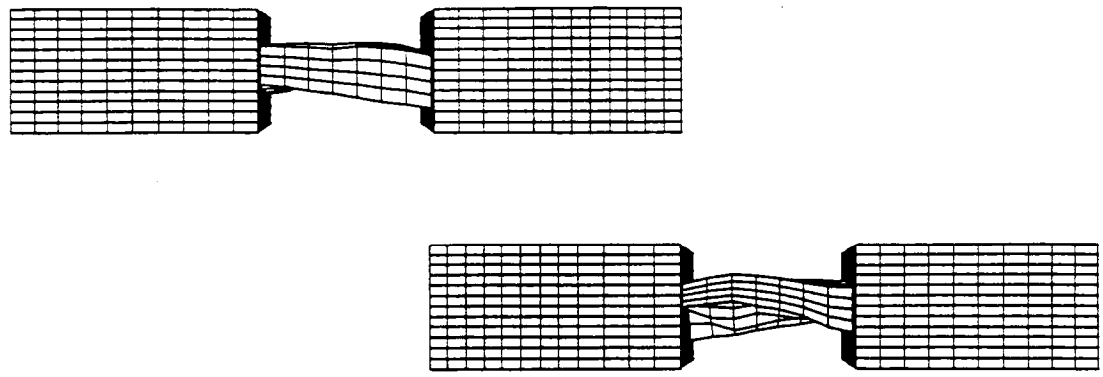

Specimen 1

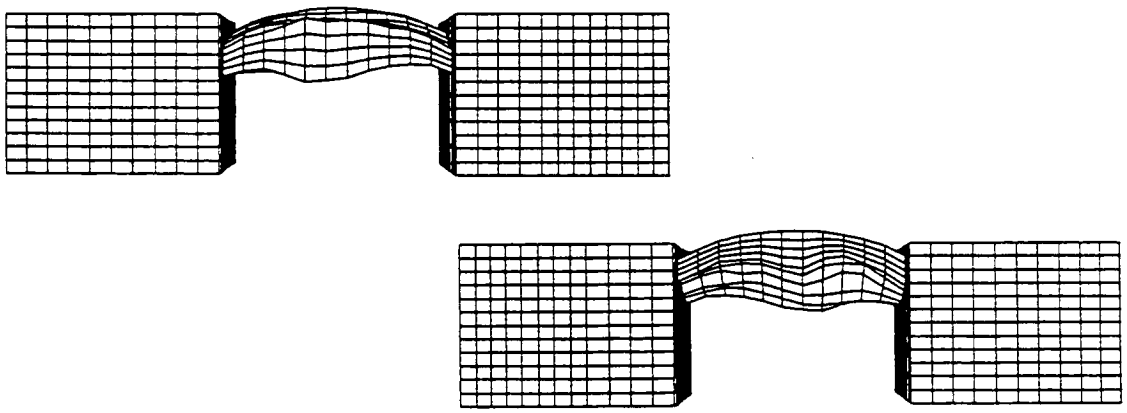

Specimen 2

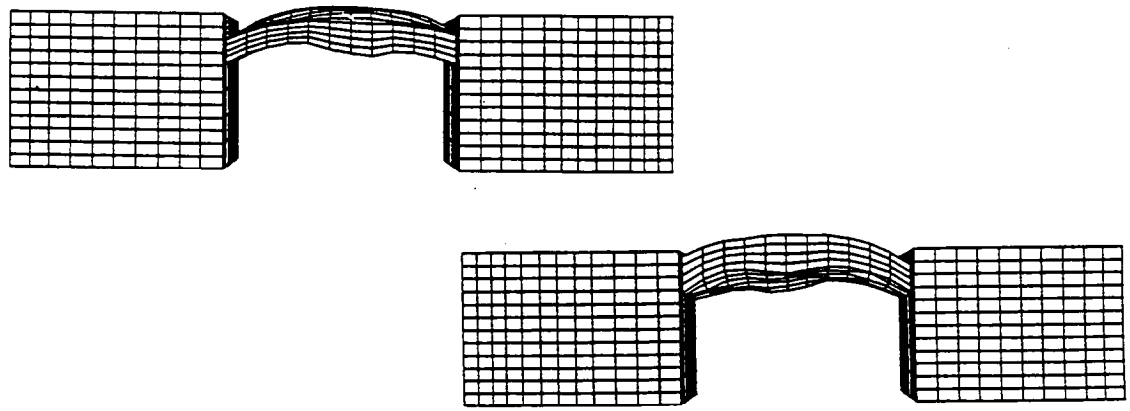

Specimen 3

Figure 4. Reconstructed occipital Bone Specimens 1, 2, and 3 imbedded in polyester castings. To illustrate the three-dimensional geometry, two views are presented for each specimen. The horizontal dimension of each bone element represents 0.508 cm.

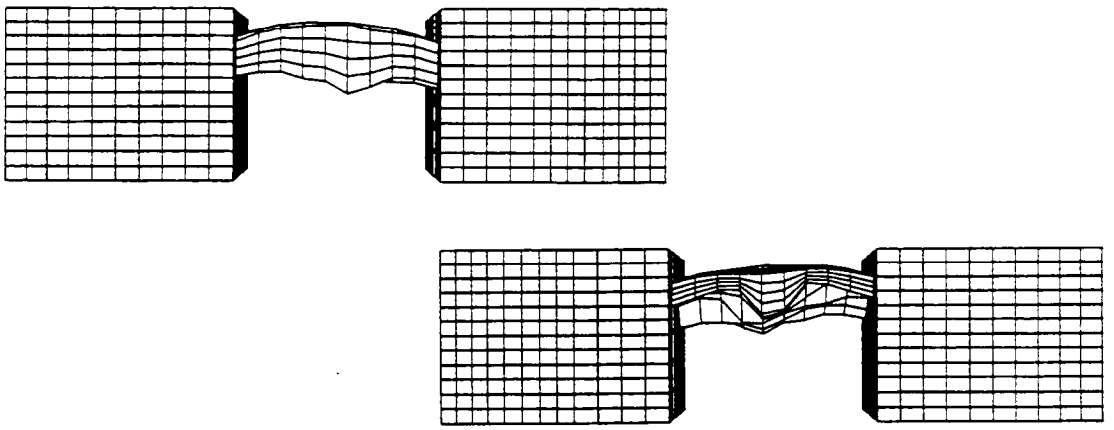

Specimen 4

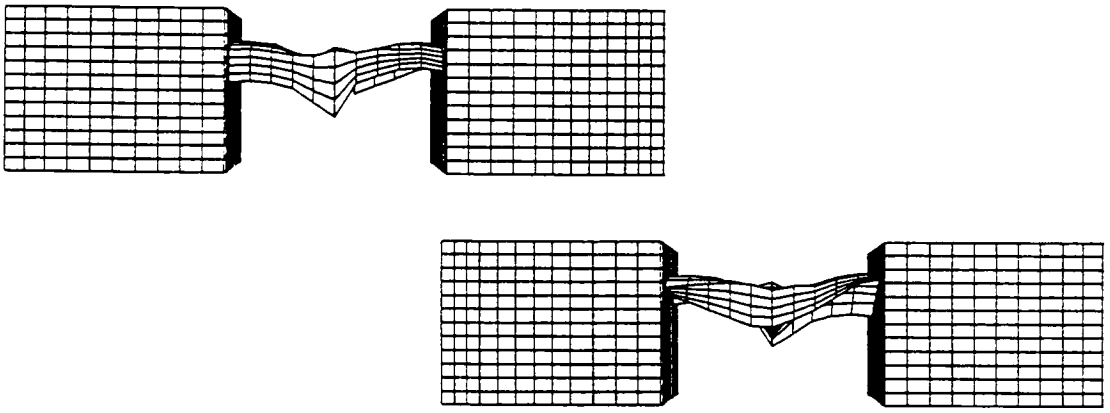

Specimen 5

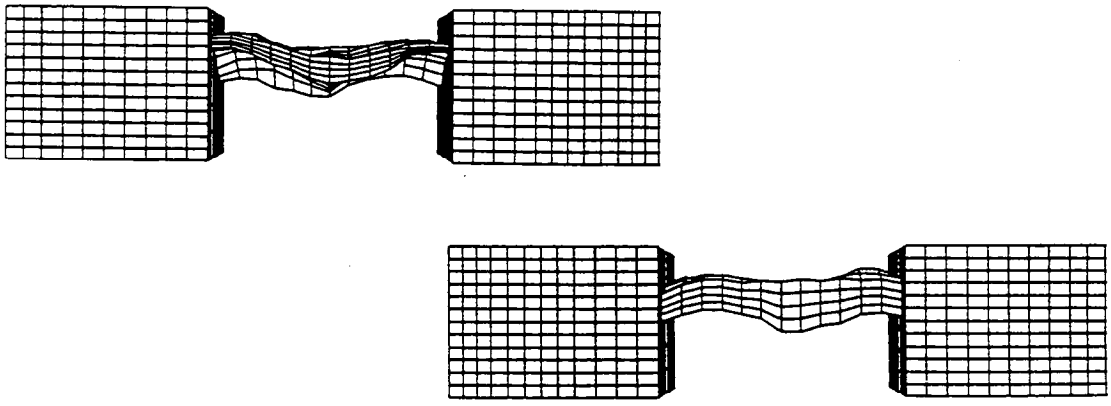

Specimen 6

Figure 5. Reconstructed occipital Bone Specimens 4, 5, and 6 imbedded in polyester castings. To illustrate the three-dimensional geometry, two views are presented for each specimen. The horizontal dimension of each bone element represents 0.508 cm.

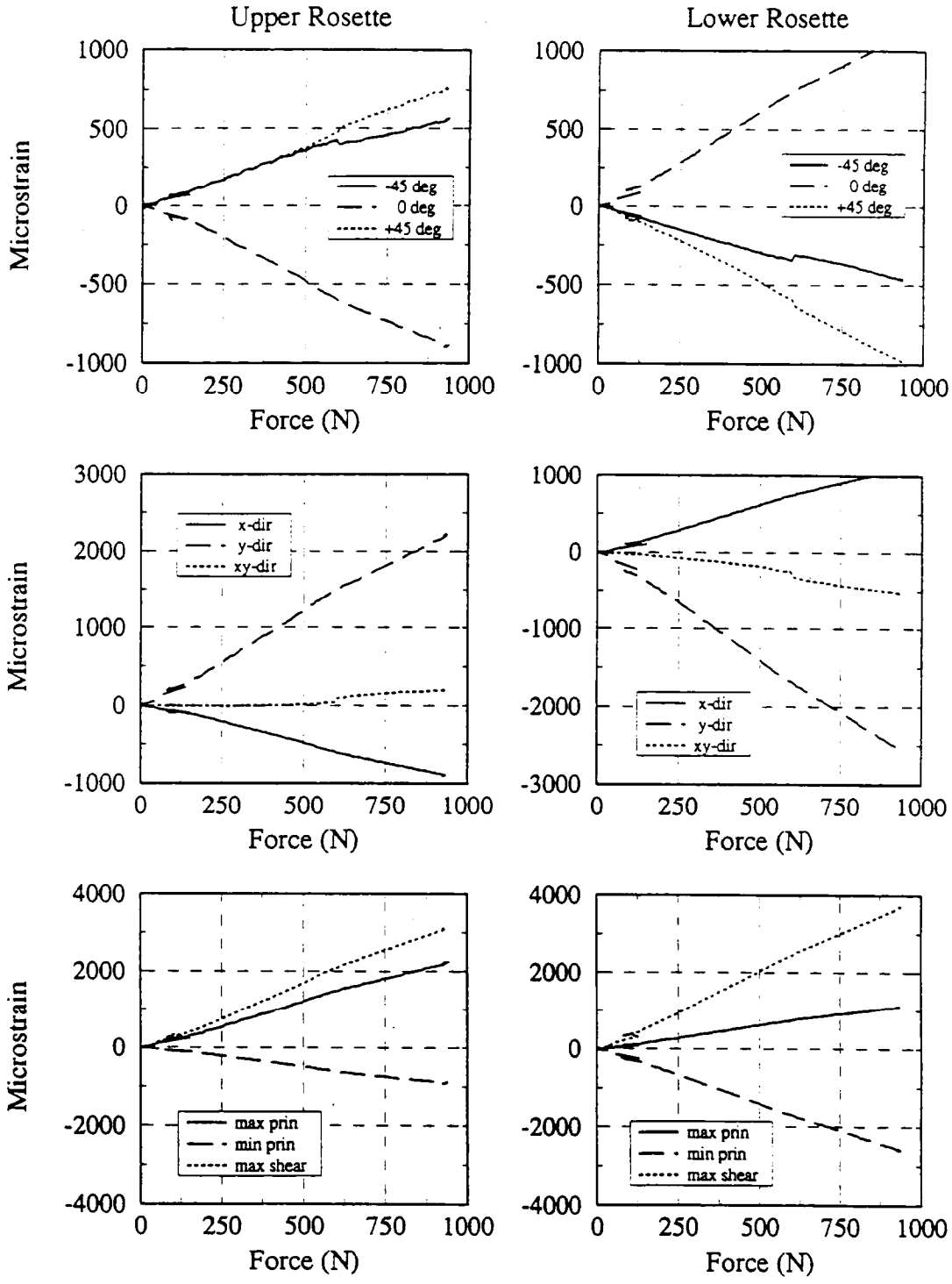

Figure 6. Force-strain data for rosettes bonded to the upper and lower surfaces of Bone Specimen 1. Data is reported to peak force for the loading phase.

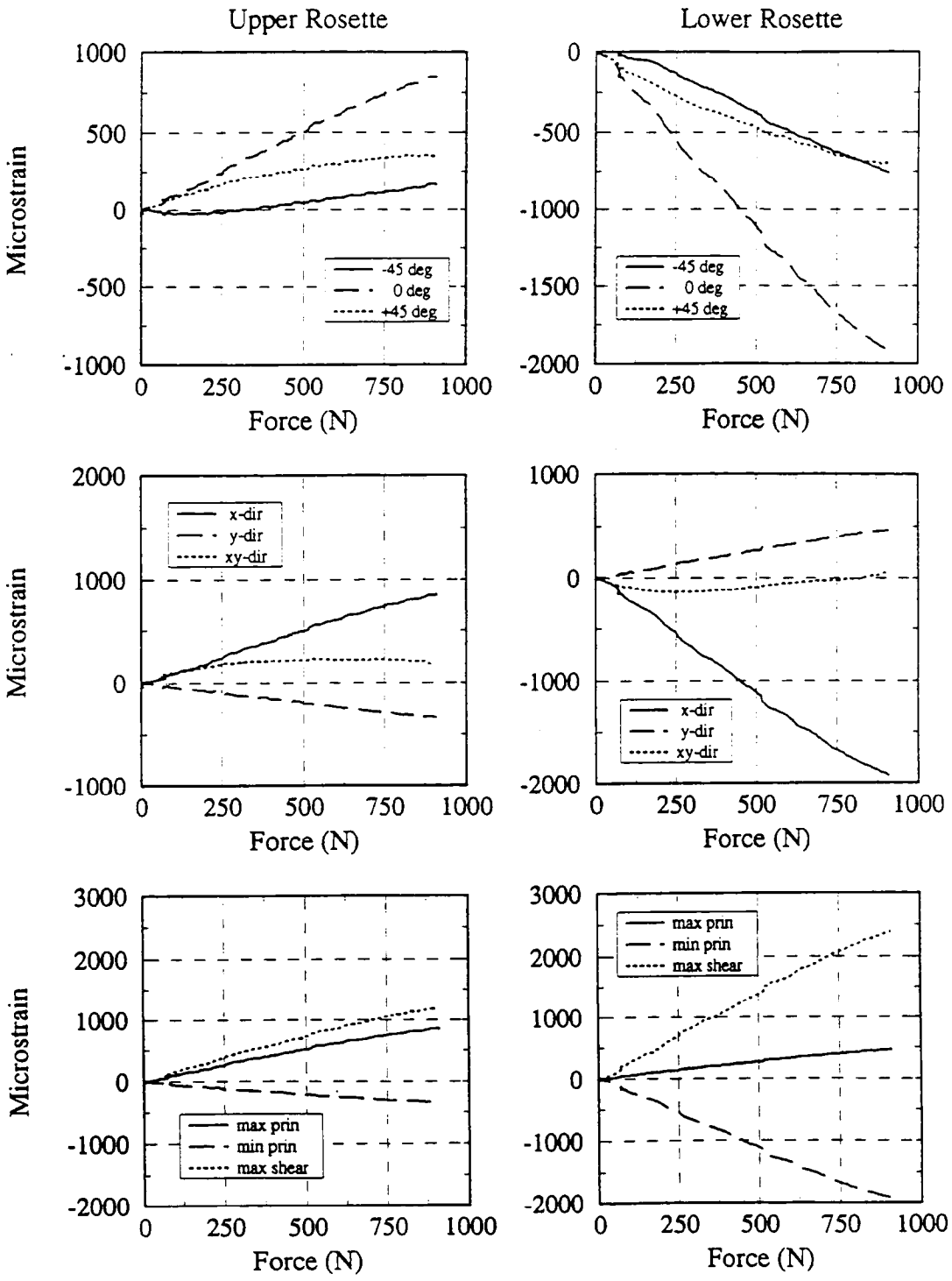

Figure 7. Force-strain data for rosettes bonded to the upper and lower surfaces of Bone Specimen 2. Data is reported to peak force for the loading phase.

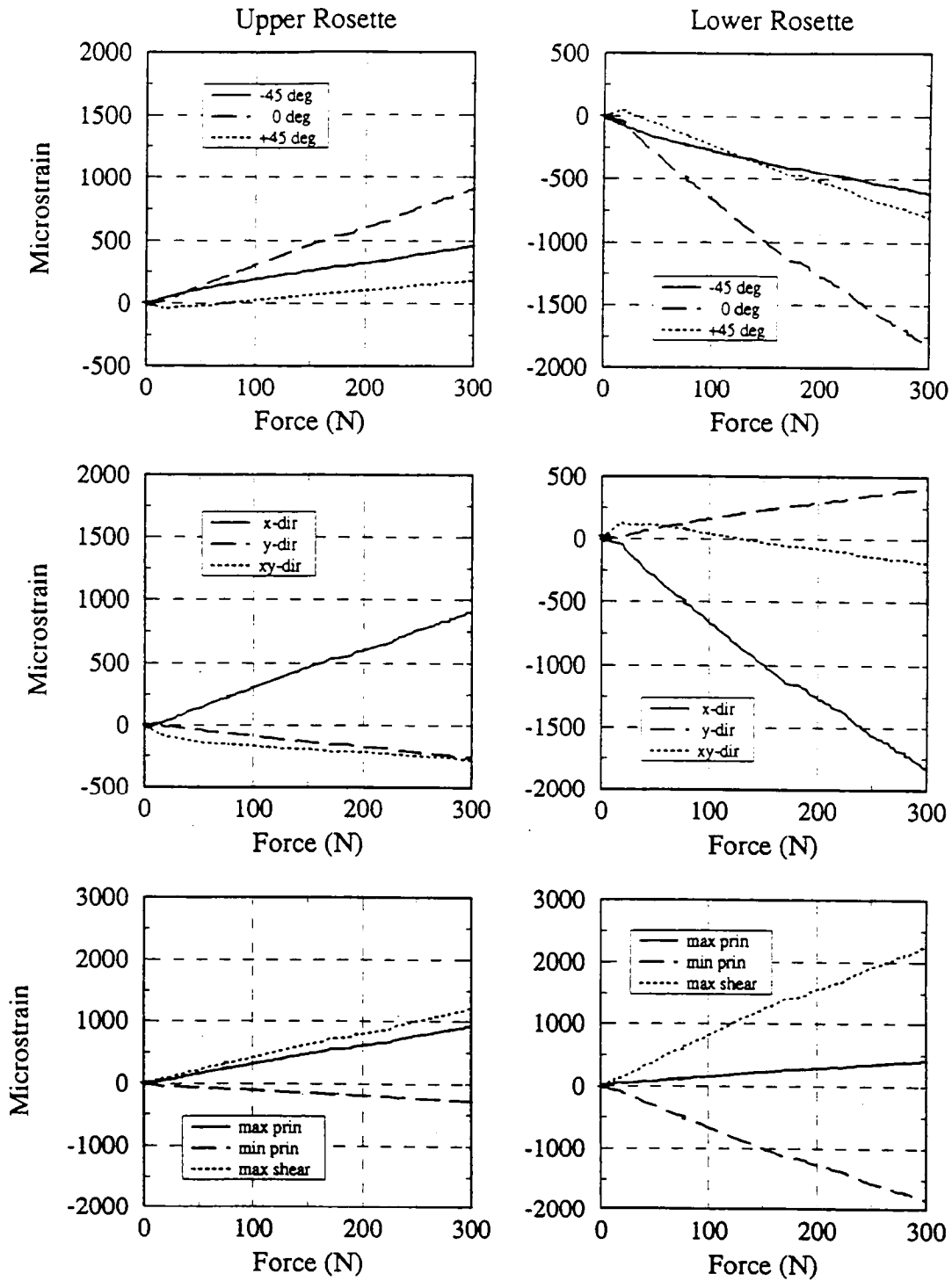

Figure 8. Force-strain data for rosettes bonded to the upper and lower surfaces of Bone Specimen 3. Data is reported to peak force for the loading phase.

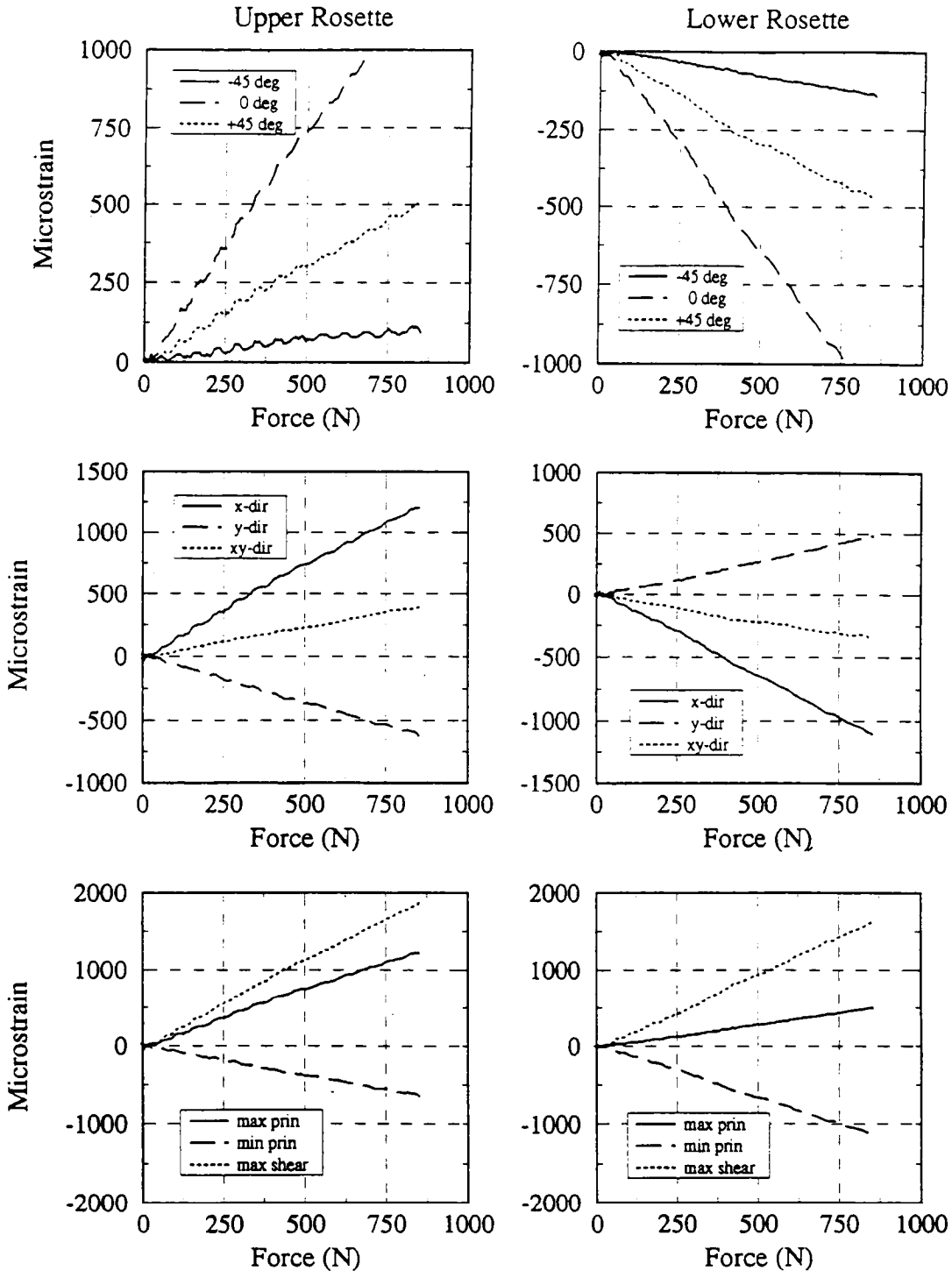

Figure 9. Force-strain data for rosettes bonded to the upper and lower surfaces of Bone Specimen 4. Data is reported to peak force for the loading phase.

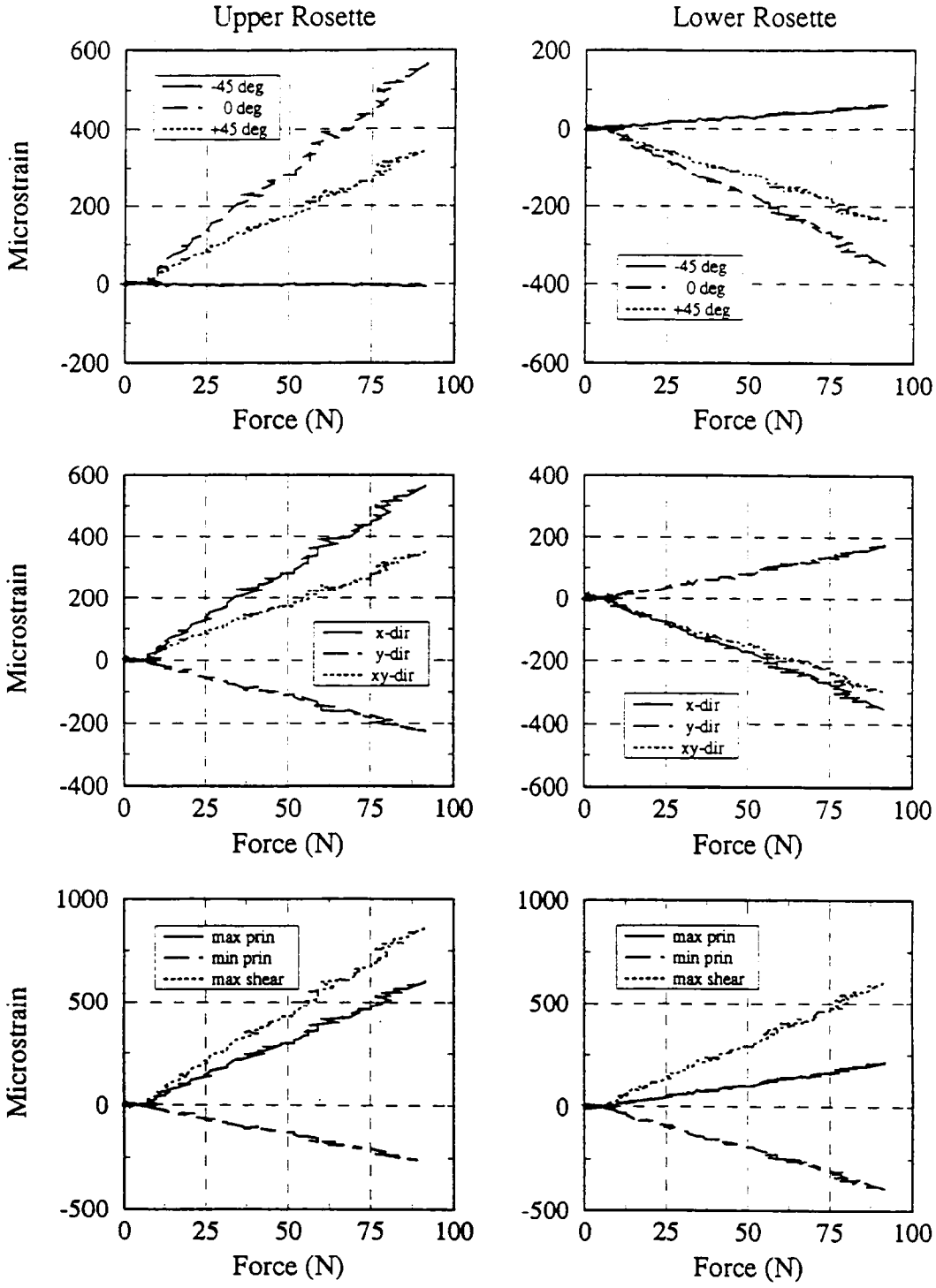

Figure 10. Force-strain data for rosettes bonded to the upper and lower surfaces of Bone Specimen 5. Data is reported to peak force for the loading phase.

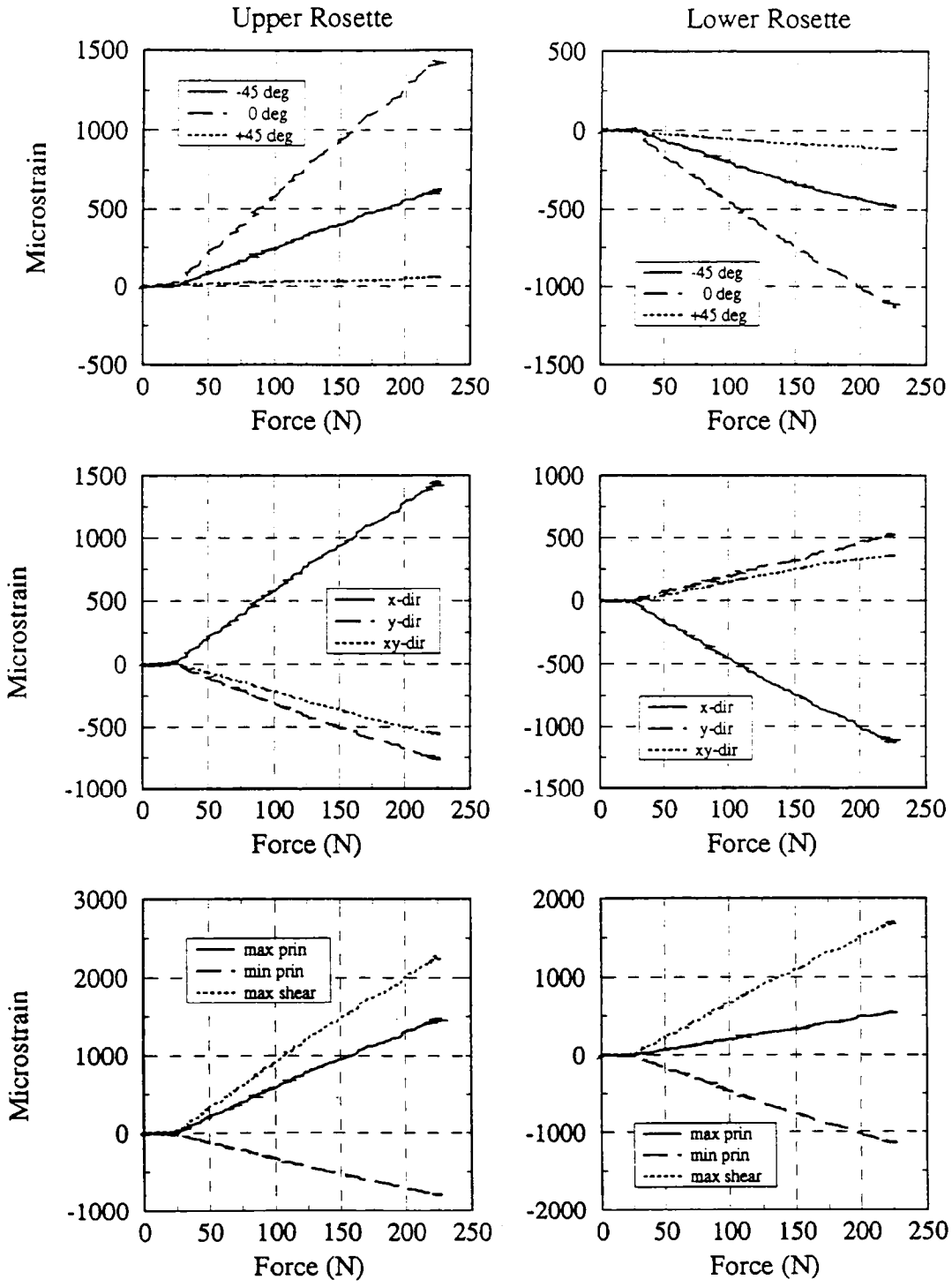

Figure 11. Force-strain data for rosettes bonded to the upper and lower surfaces of Bone Specimen 6. Data is reported to peak force for the loading phase.

Table 1. A Comparison of Principal Strains Based on Experimental Data and Finite Element Simulations

Bone Specimen	Rosette	Maximum Principal Strain			Minimum Principal Strain		
		Exp (με/Nm)	FEM (με/Nm)	Error (%)	Exp (με/Nm)	FEM (με/Nm)	Error (%)
1	Upper	197	217	9.80	-83.1	-93.4	12.4
1	Lower	98.7	88.3	-10.6	-222	-199	-10.7
2	Upper	65.2	75.7	16.1	-24.6	-23.8	-3.28
2	Lower	34.5	35.1	1.80	-149	-123	-17.5
3	Upper	194	219	12.9	-55.4	-51.7	-6.72
3	Lower	82.6	86.5	4.86	-379	-343	-9.44
4	Upper	109	116	6.29	-57.7	-53.6	-7.17
4	Lower	49.0	52.5	7.21	-106	-95.9	-9.28
5	Upper	445	430	-3.34	-194	-213	10.1
5	Lower	156	140	-9.81	-287	-302	5.28
6	Upper	465	500	7.56	-251	-239	-4.74
6	Lower	178	186	4.22	-366	-331	-9.26

Table 2. Occipital Bone Material Properties Summary

Test	Disp Rate (cm/s)	Elastic Modulus (GPa)	Poisson's Ratio	Average Absolute Error (%)	Average Squared Error (%)	Weighted Absolute Error (%)	Weighted Squared Error (%)
1	0.664	13.5	0.40	10.9	10.9	10.6	10.6
2	0.664	25.0	0.29	9.66	12.0	13.9	15.2
3	0.0600	15.0	0.23	8.48	9.00	9.64	9.95
4	0.674	22.0	0.40	7.65	7.71	7.79	7.86
5	0.0451	14.0	0.36	7.14	7.71	6.00	6.65
6	0.0418	12.0	0.45	6.53	6.89	7.12	7.41

Table 3. Material Properties from Beam Theory and Finite Element Methods for an Isotropic, Linearly Elastic Model of Occipital Bone

Bone Specimen	Elastic Modulus (GPa)			Poisson's Ratio		
	Beam Bending		Finite Element Model	Beam Bending		Finite Element Model
	Upper Rosette	Lower Rosette		Upper Rosette	Lower Rosette	
1	15.1	9.36	13.5	0.42	0.44	0.40
2	19.1	13.8	25.0	0.38	0.23	0.29
3	15.6	12.5	15.0	0.28	0.22	0.23
4	22.6	3.20	22.0	0.53	0.46	0.40
5	18.2	8.47	14.0	0.43	0.54	0.36
6	18.9	8.97	12.0	0.54	0.49	0.45

Discussion

The polyester resin specimen tests served two functions. They were used to determine the material properties of the polyester, which were subsequently incorporated in the finite element models of the bone specimens, and they also allowed an evaluation of the fixturing's ability to impose a pure moment. Since the resin specimen geometry was uniform, beam theory predicts that the strains measured on the upper and lower surfaces should be identical. If the gauges were exactly aligned along the axis of the specimen, the gauges positioned at +45 and -45 degrees should also exhibit identical behavior. Furthermore, the shear strain computed from the rosette data should be identically zero. Examining the mechanical responses of the resins, the +45 and -45 degree gauges have virtually identical slopes. The calculated shearing strain is also very close to zero for both specimens. While the slope of the shearing strain for Resin Specimen 1 is nearly zero, there is a slight offset resulting from a small torsional load stemming from misalignment between the surface of the resin specimen and the knife-edge supports. For the second resin specimen, the knife-edge supports and surfaces of the resin specimen appear to be parallel based on the absence of any initial offset in the experimental strain data. Yet a small shearing strain arises during the course of the test. The principal strains exhibit very similar trends although the strains from the lower rosette are slightly larger in magnitude than those from the upper rosette. While beam bending equations would predict identical strains for both surfaces, curved beam considerations would dictate a larger strain on the lower surface.

In all bone specimen tests, experimental force-strain curves during loading displayed strongly linear behavior with correlation coefficients typically exceeding 0.999 for linear regressions when the measured force resulted in a signal that substantially exceeded the noise from the load cell. In view of the linear behavior exhibited by the resins and bone specimens over the range of strains and loading rates considered in this study, linear elastic models were used to represent the polyester and bone material properties. Since the material properties were assumed to be linear, only a single slope parameter was necessary to represent each experimental trace. As a consequence, a regression analysis was performed over the largest linear portion of the loading curve. This technique had the advantage of excluding transient inertial loading associated with the acceleration of the ram to a constant velocity and subtle re-alignment of the specimen and fixturing at the onset of a test. If the knife-edge support and resin surface were not exactly parallel, small torsional loads were applied to the specimen at the beginning of the test. The influence of these torsional loads and the inertial artifacts could be eliminated by omitting the initial portion of the force-strain curve from the regression analysis on the basis of linear superposition.

Although there is substantial inter-specimen variation, the material property parameters for a particular bone specimen derived from elementary beam bending equations often do not agree well with the results from the finite element simulations. Beam theory also results in a consistently lower value for Young's Modulus using the strain data from the rosette on the lower bone surface. Based on this observation, the application of curved beam theory might result in better agreement between analytically determined material properties and finite element simulations. Yet even curved beam theory cannot account for the influence of local geometric variations which appear to dominate the stress and strain fields in the finite element models. To

illustrate the effects of bone geometry, Figure 12 depicts the Von Mises stress distribution predicted for Bone Specimen 4 based on optimal isotropic, linearly elastic material properties derived from the finite element simulations. As the figure illustrates, stress concentrations are most pronounced in regions where the cross-sectional geometry of the specimen varies.

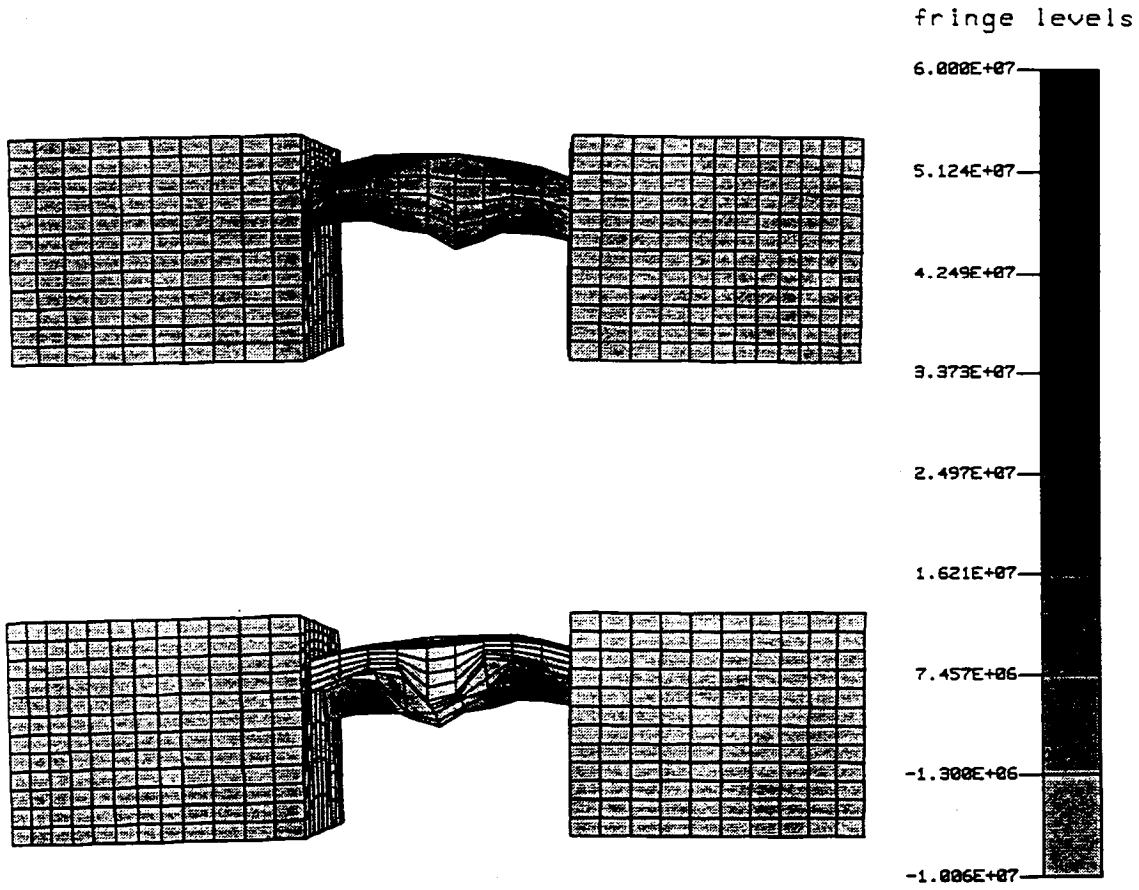

Figure 12. Von Mises stress distribution for Bone Specimen 4 viewed from both sides of the specimen. Stress concentrations are most pronounced in regions where variations in the cross-sectional geometry of the specimen occur. Stress values are reported in Pascals and the displacement scale factor is unity.

Since material properties were determined by iteratively adjusting the modulus and Poisson's ratio, adequate validation required that the number of validation parameters exceed the number of undetermined variables in the model by at least one. In the present study, the material was characterized by two constants while the principal surface strains derived from the experimental data afforded four validation quantities. To determine the five material constants associated with a transversely isotropic material model, principal strain directions could be evaluated to increase the number of available experimental parameters to six using the present data. To increase the number of validation parameters required for more complex material models, two strategies are available. To generate additional data from a limited number of

gauges, several loading schemes could be employed. Alternately, multiple rosettes could be incorporated to reduce the number of loading cases and increase the number of validation parameters derived from a single test.

While the strain data obtained from uniform, rectangular polyester test specimens indicate that the four-point bending apparatus could impose a nearly pure moment, there are several sources of error that should be considered. Although the region of load application was well-defined, the irregular geometry of the bone specimens created the possibility that the load was not uniformly distributed across each of the support surfaces. The knife-edge supports could also introduce frictional loads tangent to the surface of the specimen as the imposed displacements resulted in specimen deformation. The polyester specimen tests indicated that this latter effect was minimal when the ratio of specimen height to width was small, but the bone specimen resin blocks where the loads were applied had a height to width ratio of 0.50 in the first bone specimen test and 0.75 in subsequent tests. To minimize frictional effects, small displacements should be utilized.

The principal strains calculated from the experimental rosette data were also based on a spatial average of the surface strains. Since the planar rosette gauges covered a surface area measuring 7.14 mm x 2.38 mm, and each mesh element measured 5.08 mm x 5.08 mm, rosettes overlapped at least two neighboring elements. Although gauges were mounted on smoothly curved portions of the bone, average principal strain variations among neighboring surface elements in those regions still amounted to as much as 30%. Consequently, to attain a more localized strain assessment, stacked rosettes were used in subsequent tests that covered a surface area measuring 3.17 mm x 2.24 mm and could be placed entirely within the surface boundaries of a single mesh element.

Perhaps the largest source of error stemmed from the modeling assumptions. For the finite element models, bone was represented by a homogeneous, isotropic, linearly elastic material model. The homogeneous assumption excluded the effects of cortical and trabecular bone layers while the isotropic characterization ignored any directional dependence of the bone properties. The homogeneous assumption was not as restrictive as might be anticipated because the basilar skull bone specimens typically contained a very small trabecular layer that was sandwiched between cortical layers. Since bending tests were performed on the bone specimens, the contribution of this thin, central layer was probably less significant than it would have been in tensile or compressive tests. The experimental loading was also designed to produce a one-dimensional state of stress. As a consequence, an isotropic material model could accommodate the mechanical response of the bone specimens if the material properties were isotropic in the plane that principal surface strains were measured. Data from several investigators (McElhaney *et al.*, 1970; Reilly and Burstein, 1975; Yoon and Katz, 1979) suggest that bone is transversely isotropic with the plane of isotropy tangent to the bone surface.

In view of these modeling assumptions and experimental sources of error, the agreement between experimental and predicted principal strain values from the finite element simulations is quite good. On average, only a 10% difference was noted between experiment and simulation.

Conclusions

Based on the results from the polyester specimen tests, the experimental apparatus designed for four-point bending could apply a nearly pure moment if the test specimen was uniform and thin. The irregular geometry of the bone specimens, friction, and the constraints imposed by the knife-edge supports degraded the ability of the fixturing to impose a pure moment. Subtleties in knife-edge support and specimen surface alignment tended to introduce torsional loads but these effects were confined to the initial portion of the force-strain response. The effect of torsional loads stemming from misalignment could be excluded from the mechanical response on the basis of linear superposition.

Both the polyester resin and occipital bone specimens exhibited linear mechanical responses over the range of strains and loading rates considered in the present study, endorsing the use of linearly elastic material models. Using inverse finite element analysis and treating the bone as a homogeneous, linearly elastic, isotropic material yielded a mean Young's modulus of 16.9 ± 5.3 GPa and an average Poisson's ratio of 0.355 ± 0.081. These values are in close agreement with material properties for cortical bone derived from other locations on the skull. The error between experimentally measured surface strains and those predicted by the finite element simulations, using optimal material properties, was found to be on the order of 10% for bending. Estimates of material properties based on elementary beam theory cannot account for complex bone geometry and the material properties predicted by beam bending equations often did not agree well with the results from the finite element simulations. However, inter-specimen material property variations were also significant in the present study and tended to obscure variations stemming from the different analysis techniques.

References

Annual Book of ASTM Standards. American Society for Testing Materials, Philadelphia, Pa., 1978.

Ashman, R. B., Cowin, S. C., Van Buskirk, W. C., and Rice, J. C., "A Continuous Wave Technique for the Measurement of the Elastic Properties of Cortical Bone." *J. Biomechanics*, **17**:349, 1984.

Ashman, R. B., Corin, J. D., and Turner, C. H., "Elastic Properties of Cancellous Bone: Measurement by an Ultrasonic Technique." *J. Biomechanics*, **20**:979, 1987.

Ashman, R. B., "Experimental Techniques." in *Bone Mechanics*, Chapter 5. Cowin, S. C., Ed., CRC Press, Inc., Boca Raton, Florida, pp. 75-95, 1989.

Dechow, P. C., Nail, G. A., Schwartz-Dabney, C. L., and Ashman, R. B., "Elastic Properties of Human Supraorbital and Mandibular Bone." *Am. J. Phys. Anthropology*, **90**:291-306, 1993.

Evans, F. G. and Lissner, H. R., "Tensile and Compressive Strength of Human Parietal Bone." *J. Appl. Physiol.*, **10**:493-497, 1957.

Keaveny, T. M., Borchers, R. E., Gibson, L. J., and Hayes, W. C., "Theoretical Analysis of the Experimental Artifact in Trabecular Bone Compressive Modulus." *J. Biomechanics*, **26**:599-607, 1993.

Keaveny, T. M. and Hayes, W. C., "A 20-Year Perspective on the Mechanical Properties of Trabecular Bone." *J. Biomech. Eng.*, **115**:534-542, 1993.

McElhaney, J. H., Alem, N., and Roberts, V. "A Porous Block Model for Cancellous Bones." ASME Paper No. 70-WA1BHF-2, pp. 1-9, 1970.

Reilly, D. T., and Burstein, A. H., "The Elastic and Ultimate Properties of Compact Bone Tissue." *J. Biomechanics*, **8**:393, 1975.

Wood, J. L., "Dynamic Response of Human Cranial Bone." *J. Biomechanics*, **4**:1-12, 1971.

Yoon, H. S. and Katz, J. L., "Temperature Dependence of the Ultrasonic Velocities in Bone." *1979 IEEE Ultrasonics Symp. Proc.*, pp. 395-398, 1979.

DISCUSSION

PAPER: **Method for the Evaluation of Bone Specimen Material Properties**

PRESENTER: Robert H. Hopper, Jr., Duke University

QUESTION: Guy Nusholtz, Chrysler Corporation

It looked like you were using Aidnode brick elements for your plastics at the end. How much did you have to actually do some computation with relationship to the deformation of that plastic, or could you just set end conditions on the end of your piece of bone?

ANSWER: Yes. Because of the nature small displacement, we didn't see a lot of plastic deformation near the ends because of the thickness of the polyester resin specimens. What we simply did was attach the boundary conditions to the nodes there and impose it. There wasn't a lot of deformation restraint associated with those boundary conditions.

Q: So you didn't have to get the material properties of the plastic.

A: Actually we did include the material properties of the plastic; basically, the polyester resin, if I'm understanding your question properly. We did do that. We assessed it using polyester resin specimens and then assigned material properties to the casting blocks. The modulus turned out not to be significantly different from bone so I thought it was important to include the modulus.

Q: Did it have an effect on what your final results were?

A: Actually, we looked at varying that and we were far enough away that the change with a significant change in the modulus of the resin was very minimal, only on the order of two or three percent for the region that we were looking at: the strains on the occipital bone. So, any the modulus didn't have a significant effect on the material properties that we were measuring locally that were reasonably far away from those plaster castings.

Q: An inverse method to determine material properties is a very good way to approach things. That's been used on plastics and other type of materials but what you could be doing is tuning it. Everything's going to be locally linear unless it is catastrophic or on some sort of chaotic cusp of some nature. How do you know that ten percent is really an error as opposed to something where you've driven it by the inverse technique?

A: Right. I think within the optimization technique you struggle with the facts that are you at a local minimum? Fortunately, for the application that we used here, we had a fairly one dimensional state of stress with the nature of the imposed loading, and therefore, the material properties didn't exhibit a strong coupling.

In other words, when you chose the modulus, it determined the response along the axis. And when you determine the Poisson ratio, it was sort of the off- axis response. So there wasn't a strong coupling between those two material properties from the model that we chose. I think

that the problem becomes far more sophisticated for more complex material models.

Q: And what would you attribute the ten percent error to?

A: There are a lot of sources. First of all, we didn't have exactly pure bending. There were errors associated with quantifying the geometry and then there are, of course, the approximations. Bone in a large scale representation is probably not adequately represented by a linearly elastic homogeneous material.

In other words, the modeling that we did exclude the contribution from the trabecular bone. Admittedly, that region is small in the basilar region of the skull. It is also centrally located but I think friction and then the assumptions that underlined the type of material model that we chose are really what is contributing to the error along with some experimental uncertainty.

Q: Thank you.

A: Thank you.

Q: N. Yoganandan, Medical College of Wisconsin

A good presentation and it is very nice to see that the modulus of elasticity which you got, what about 17,000 MPA?

A: The modulus, I believe was about 16.9 GPA.

Q: Yes. I'm used to MPA, in any case. That is exactly what researchers have been using for the last twenty, thirty years on long bones where they did a bunch of experiments using a similar phenomenon as you had, putting in a bunch of strain gages and calculating the modulus of elasticity. If I remember correctly, they use about 16 GPA.

One other comment I have is, you mentioned something about using the CT-BASED density measurements for the trabecular bone. Could you comment on how would you do to have a piece of bone specimen which has got different combinations of cancellous bone which is the cortical bone and how would you estimate the density of the Young's modulus off the cortical bone using the CT scans? You can get the densities for the trabecular bone very easily, but can you comment on how would you plan on getting it for the cortical bone.

A: Yes, actually I can comment on the context of our recent applications. In a lot of our finite modeling and especially the skull model (because the size of the element is larger than the pixel in the CT scan,) we are forced to do some kind of averaging technique to determine and assign moduli values to the finite element models. So what we've been doing is actually looking at individual pixels, normalizing it to some maximizing intensity that we assume then correspond to the cortical bone, and weighting the modulus value based on the weighting within a particular finite element of the entire pixel domain.

In other words, we look at the intensity of each pixel within the domain. Assign it a

certain weighting function, based on the maximum value for cortical bone and then average all those pixel intensities to determine an average modulus value over the domain of each individual element.

Q: So you have that difference of about 200 between the trabecular bone, Young's modulus versus the cortical bone Young's modulus. In which case, if I understand you correctly, this procedure of estimating based on the pixel size, you may have some kind of an error because the thickness of the cortical bone is different for different thickness of the body so you may want to use some other technique instead of just relying on the CT density because of the mismatch of the material properties in the cortical bone and the cancellous bone.

A: Yes. Thank you. I will investigate that when we tackle that.

Q: Thanks.